

Hysteresis and packing in gas-fluidized beds

R. Ojha, N. Menon,* and D. J. Durian

Department of Physics and Astronomy, UCLA, Los Angeles, California 90095-1547

(Received 25 January 2000)

The packing fraction and the pressure drop across gas-fluidized beds of granular media exhibit hysteresis as the gas-flow rate is cycled up and down across the fluidization transition. Presumably this is due to contact forces and transfer of stress to the surrounding walls, and hence should vary nontrivially with the aspect ratio of the sample. Here we present systematic measurements of the variation of hysteresis with particle size and aspect ratio of the sample. Remarkably, the hysteresis scales in a trivial way with these parameters, showing no evidence of long-range effects of the wall. Our measurements also show that the packing fraction becomes 0.590 ± 0.004 , independent of particle size and container shape, when the fluidizing flow of gas flow is slowly removed.

PACS number(s): 83.70.Fn, 45.70.-n, 47.55.Kf

I. INTRODUCTION

In the absence of sufficiently strong external forces, granular materials are “jammed” in the sense that individual grains are locked forever into some random packing configuration set by the most recent flow history [1]. Since thermal energies are far too small to overcome gravity, there is no relative motion of grains and no relaxation of shear stresses. The medium is thus a solid, albeit an unusual one [2]. Stress heterogeneities can organize and correlate over long distances in the form of “force chains,” complicating the application of continuum elasticity theory. These can vault across the sample and transfer weight to the vertical container walls, giving rise to such characteristic granular behavior as the saturation of hydrostatic pressure in a silo that is deeper than it is wide. The stress heterogeneities can also exhibit construction history dependence, as in whether or not a dip in normal force occurs under the center of a conical pile of sand [3].

The unusual properties of a granular solid are reflected in unusual transitions to a granular fluid upon application of external forces. This includes intermittent avalanches down the surface when tilted, convection and pattern formation when shaken, and bubbling and hysteresis when subjected to an upflow of gas (counter to gravity). Here we focus exclusively on the latter, about which much is already widely known [4–6]. For low flow rates, the gas percolates upwards through the static packing of grains with a net pressure drop ΔP that increases with the superficial gas velocity, $U_s = Q/A$, where Q is the volume flow rate and A is the cross-sectional area of the sample. The Ergun equation [4–6] gives an accurate correlation between pressure gradient and flow rate in terms of the particle size, shape, and packing density, as well as the gas viscosity and density. At progressively higher flow rates, more and more of the weight of the material is supported by the pressure drop in the gas. When ΔP reaches the total weight of material per unit area, mg/A , all weight is supported by the gas, none by contact forces or the walls, and the system is said to be fluidized. At even higher

gas-flow rates, the pressure drop remains pegged at mg/A due to a fixed fraction of gas percolating up through the grains and all the rest escaping in the form of large gas bubbles. If the grains are sufficiently large and heavy, then bubbling begins immediately at the onset of fluidization and there is no hysteresis when the gas-flow rate is ramped back down. This is commonly known as “Geldart B” (bubbling) fluidization behavior. By contrast, if the grains are sufficiently small and light, then there can be an interval of “uniform fluidization” between first fluidization and onset of bubbling. This is known as “Geldart A” (aeratable) behavior and is accompanied by hysteresis in pressure drop and bed height as the gas-flow rate is cycled back down [7]. A curious feature is that the so-called “uniform fluid” is not actually a fluid at all, since density heterogeneities do not relax [7] and since there is no relative grain motion whatsoever [8]. Macroscopically it appears fluidlike in that it presents little if any viscous resistance to being stirred, and it sloshes around if bumped. Nevertheless, it must be a rather fragile solid that yields and flows, seemingly without viscosity, in response to small forces. Such a state of matter is highly unusual indeed.

In an attempt to gain insight into the “uniform fluid,” we made extensive study of the hysteresis in pressure and bed height that accompanies its existence. Since gas fluidization involves transfer of weight away from contact forces between grains and the surrounding walls, and since the latter are important only for deep samples, we supposed that hysteresis would be influenced by the aspect ratio of the sample. An explicit calculation of such an effect is given in Ref. [9]. Therefore, we report here observations of hysteresis as a systematic function of both container shape and filling depth. To our surprise, no interesting dependence was found. To our further surprise, when the upflow of gas was gradually removed, a packing fraction of 0.590 ± 0.004 was always recovered, independent of both system size and grain size. These observations have important implications for our understanding of both gas fluidization and packing behavior in granular media.

II. MATERIALS AND METHODS

For our study we used monodisperse glass beads of four different diameters, 50, 100, 200, and 350 μm , all with a

*Now at the University of Massachusetts, Amherst, Department of Physics and Astronomy.

size dispersion of about 5% [10]. The corresponding mass densities of the glasses are $\rho=2.35, 2.40, 2.44,$ and 2.50 g/cm^3 , all to within $\pm 0.01 \text{ g/cm}^3$. According to Geldart's classification scheme, for this density the boundary between type *A* and type *B* behavior is at $120 \mu\text{m}$. Thus, large hysteresis is expected for the $50 \mu\text{m}$ beads, less for the $100 \mu\text{m}$ beads, and none for the 200 and $350 \mu\text{m}$ beads. Prior to use, the beads are dried thoroughly by baking in air or in vacuum; afterwards, a continuous flow of N_2 gas up through the bed keeps the beads dry and also removes fines.

Fluidized beds were constructed from precision-bored cylindrical glass tubes of three different diameters, $D=0.5, 1,$ and 2 in. One end is open to the atmosphere, and the other is mounted to a sintered glass frit, which serves to uniformly distribute the gas. Together, the frit and tube are sealed onto a large windbox with one port for introducing the gas and one port for measuring the pressure. This is a standard design [7], similar to that in our previous study [8].

For each experiment, a known mass m of glass beads is poured into the tube and three quantities are measured as the flow rate Q of dry N_2 gas is cycled up and down. First, Q is obtained from carefully calibrated floating-ball rotameters. Dividing by the tube area, this gives the superficial gas-flow speed, $U_s=Q/A$, as noted above. Second, the total pressure drop of gas across the frit and bed is obtained by a transducer. Subtracting off the pressure drop across the frit, measured previously with an empty tube at all relevant flow rates, this gives the pressure drop ΔP across the granular medium. Third, the bed height H is obtained visually from a clear ruler taped to the outside of the glass tube. Taking a ratio of volumes, this gives the packing fraction of solids as $\phi=(m/\rho)/(AH)$.

III. RESULTS

Hysteresis loops for both pressure drop ΔP and bed height H are shown in Fig. 1 for $D=1$ -in.-diam fluidized beds. This includes three bead sizes (data were not taken for the $200 \mu\text{m}$ beads), and several aspect ratios H_o/D . The loops shown as solid curves all represent reproducible cycles, independent of initial conditions, with behavior as follows. At low flow rates the height is constant, H_o , and the pressure increases monotonically with the flow rate. When the flow rate exceeds a certain threshold at, or near, fluidization, the bed suddenly expands and the pressure correspondingly drops. At higher flow rates the pressure does not increase appreciably, but the bed continues to expand, at first to achieve a lower packing density but later to accommodate the excess gas rising as bubbles. As the gas flow is ramped back down, the pressure and height curves are reversible as long as bubbles still exist. At lower rates, once bubbling has ceased, the height gradually decreases to the same constant value, H_o , and the pressure gradually decreases to zero, but along curves that differ from those for increasing flow rates. If the flow rate is cycled up and down, the same solid curves are retraced. The dashed curve at the upper left, for the smallest beads and the largest aspect ratio, represents initial behavior. When beads are first poured into the tube, the height is less than H_o and this denser packing leads to a higher pressure drop. After first expansion, the behavior becomes reproducible, joining the retraceable hysteresis loops.

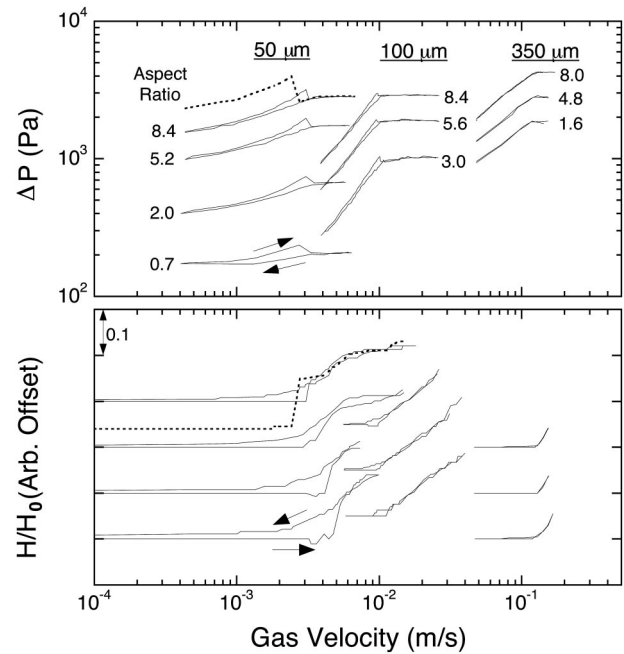


FIG. 1. Typical data for gas-pressure drop and bed height vs superficial gas velocity. Solid curves represent retraceable hysteresis loops, in the direction indicated. The dashed curve represents initial behavior, as the flow rate is ramped up for the first time for beads freshly poured into the tube. Results are for the 1-in.-diam bed, with bead sizes and aspect ratios (height to diameter) as labeled.

Several expected features can be seen in the data of Fig. 1. First, the gas speed required for fluidization depends on particle size but not on bed height. Larger particles require larger flow speeds since the interstitial space is larger, making the gas shear rate, and hence the viscous drag force, correspondingly smaller. And since both the total mass and the pressure drop at fixed flow rate scale in proportion to bed height, the same flow speed is required for all heights. Second, the size of the hysteresis loops decreases with increasing particle size and vanishes altogether for the largest diameter beads, in accord with the Geldart classification scheme.

The principal unexpected feature in Fig. 1 is that the size of the hysteresis loops scales trivially in proportion to the bed height H . Since the data are presented on a log-log plot, this is evident by the equal areas in the display, independent of bed height. Only slight differences can be perceived, but these are not systematic with bed height and arise only because the gas velocity was not incremented in arbitrarily fine steps. The same trivial scaling was observed also for the other two diameter tubes, $D=0.5$ and 2.0 in. Since at zero flow rate the hydrostatic pressure increases with depth only down to a distance comparable to the tube diameter, below which weight is supported by contact forces with the wall, we expected to find different behavior for short beds with $H < D$, where the walls play no role. For example, we expected the hysteresis loop area to scale with H only for $H \gg D$, perhaps with D/H corrections otherwise. Obviously such behavior was not found and can be ruled out. This has important implications. Namely, wall effects are unimportant below the onset of fluidization. All the weight is supported by a combination of hydrostatic pressure, as in an ordinary

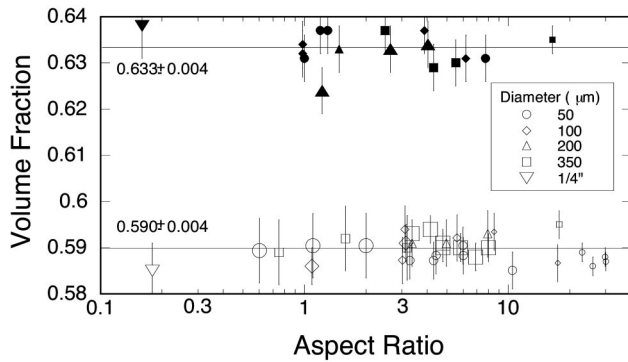


FIG. 2. Solids packing fraction as a function of aspect ratio for glass beads freshly poured into the tube (solid symbols) and following a cycle of fluidization (open symbols). Bead diameter is denoted by symbol shape, as labeled, and tube diameter is denoted by symbol size, monotonically increasing for the 0.5-, 1-, and 2-in. tubes. The error bars denote statistical error in the bed height measurement, $\Delta\phi = \phi\Delta H/H$, due to a resolution of $\Delta H = 0.5$ mm. Packing fractions for 1/4-in.-diam hollow polypropylene spheres in an 8.5-in.-diam tube are also included. Note that the packing fractions exhibit no dependence on aspect ratio or bead size; average values are denoted by the solid lines.

solid or liquid, and the upflow of gas.

We have found identical behavior for a petroleum cracking catalyst powder (Englehard Corp., NJ) composed primarily of kaolin clay and silica. Namely, the size of the reproducible hysteresis loop for pressure vs flow rate scales in direct proportion to container height, as though support of weight through contact with the walls were unimportant. This was verified for 2-in. diam beds filled to aspect ratios of 0.75, 2, 5, 7, and 10.

As an aside, note that these experiments are not easy in that many sources of experimental error could give rise to a false signal, i.e., one with $1/H$ corrections to trivial scaling. Possibilities include, most obviously, an additive error in measurement of the bed height or pressure drop. The former could arise easily from misjudging the depth of the frit, which is hidden within a flange. The latter could easily arise from error in subtracting the pressure drop across the frit, which in fact accounts for most of the measured pressure drop. As we found in preliminary runs, false $1/H$ artifacts can also arise from geometric irregularities in the bed construction, such as gaps or occlusions where tube meets frit, a tube area that varies slightly with height, or a tilting of the tube away from vertical. We also found that a false $1/H$ artifact can arise from static electricity immobilizing a layer of grains against the wall, or from miscalibration of the gas-flow meters. Altogether, if there is a true residual $1/H$ effect lurking in the statistical noise of our hysteresis loop data, it must be small and will be very difficult to demonstrate convincingly.

And finally, there is another unexpected feature in our data to which we would like to call attention. This regards the solids packing fraction, which may be extracted from the bed height as noted in Sec. II. Results are displayed in Fig. 2 for all four bead sizes, and for all three tube diameters, as a function of aspect ratio. The upper set of data (closed symbols) is from the initial bed height, after the beads were poured into the tube but before any fluidization. The data are spread around a constant value of 0.633 ± 0.004 , with no dis-

cernible trends. This agrees with the accepted value of “random close packing,” 0.637 [11,12]. The lower set of data (open symbols) is from the reproducible static bed height H_0 , obtained after slowly removing the fluidizing gas. These data are spread around a constant value of 0.590 ± 0.004 , again with no discernible trends. This value is the puzzle. It is slightly looser than the original “random loose packing” value of 0.601, obtained by tipping a container on its side, slowly rotating, and gradually returning it to upright [11]. And it is slightly denser than simulated loose packings of 0.58, obtained by adding beads one at a time to local minima at the bed surface [13,14]. We also find the same packing fractions for 1/4-in.-diam hollow polypropylene balls (Engineering Laboratories Inc., Oakland, NJ). There have been at least two earlier experiments reporting the same packing fraction, 0.59, that we find reproducibly upon cessation of fluidization. In Ref. [15], final packing densities are reported for 250- μm -diam glass spheres that were sheared, or allowed to sediment, in fluids of varying density. For experiments in air, packing fractions of 0.595 ± 0.004 and 0.585 ± 0.005 are found, respectively, for sedimentation and steady shear. When submerged in density matching fluids, the packings became looser and approached 0.555 ± 0.005 in the limit of zero density difference. In Ref. [16], packing densities of 2-mm-diam glass beads are reported vs time as the system is subjected to vertical vibration. To obtain a reproducible starting condition, dry N_2 gas was first flushed up through the column. Such fluidization gave reproducible packing densities between 0.58 and 0.60. Combined with our observations, these findings suggest that there is a common, well-defined, widely reproducible, post-fluidization “random loose packing” structure that deserves further study (number of contacts per grain, pair correlation function, etc.). It is random, but looser than random close packing, and yet has considerable stability against earth’s gravity.

IV. CONCLUSION

To reiterate, we searched for a nontrivial aspect ratio dependence in the pressure and bed height hysteresis loops for gas-fluidized beds. None was found. This null result is surprising, because it suggests that wall effects are completely unimportant in the transition from solid to fluid. Even though the walls support weight in the absence of gas flow, all weight is supported by the sum of hydrostatic contact forces and gas-pressure gradient near the onset of fluidization. Hence there is no significant vaulting of force chains, and continuum descriptions of the fluidization processes and the bubbling instabilities should be applicable. Furthermore, we found that our grains, after having been fluidized, configure into a packing structure with a solids volume fraction of 0.59, for all grains sizes, all tube diameters, and all aspect ratios. This number has been reported previously, but its ubiquity was not suspected. Its value, and the packing structure itself, must be understood if we are to develop a complete understanding of fluidization and yielding phenomena in granular materials.

ACKNOWLEDGMENTS

We thank David Goldfarb and Gary Grest for helpful conversations. This work was supported by NSF through Grant No. DRM-9623567 and by NASA through Grant No. NAG3-1419.

- [1] A.J. Liu and S.R. Nagel, *Nature (London)* **396**, 21 (1998).
- [2] H.M. Jaeger, S.R. Nagel, and R.P. Behringer, *Rev. Mod. Phys.* **68**, 1259 (1996).
- [3] L. Vanel, D. Howell, D. Clark, R.P. Behringer, and E. Clement, *Phys. Rev. E* **60**, R5040 (1999).
- [4] J. F. Davidson, R. Clift, and D. Harrison, *Fluidization* (Academic Press, London, 1985).
- [5] D. Geldart, *Gas Fluidization Technology* (Wiley, New York, 1986).
- [6] D. Gidaspow, *Multiphase Flow and Fluidization* (Academic Press, Boston, 1994).
- [7] S.C. Tsinontides and R. Jackson, *J. Fluid Mech.* **255**, 237 (1993).
- [8] N. Menon and D.J. Durian, *Phys. Rev. Lett.* **79**, 3407 (1997).
- [9] R. Jackson, in *Fluidization IX: Proceedings of the Ninth Engineering Foundation Conference on Fluidization*, edited by L.-S. Fan and T. M. Knowlton (Engineering Foundation, New York, 1998), pp.1–13.
- [10] Cataphote Inc., Jackson MS.
- [11] G.D. Scott, *Nature (London)* **188**, 908 (1960); see also G.D. Scott and D.M. Kilgore, *J. Phys. D* **2**, 863 (1969).
- [12] D. J. Cumberland and R. J. Crawford, *The Packing of Particles* (Elsevier, New York, 1987).
- [13] S.C. Reyes and E. Iglesia, *Chem. Eng. Sci.* **46**, 1089 (1991).
- [14] J. Cesarano (private communication).
- [15] G.Y. Onoda and E.G. Liniger, *Phys. Rev. Lett.* **64**, 2727 (1990).
- [16] J.B. Knight, C.G. Fandrich, L. Chun Ning, H.M. Jaeger, and S.R. Nagel, *Phys. Rev. E* **51**, 3957 (1995); see also E.R. Nowak, J.B. Knight, E. Ben-Naim, H.M. Jaeger, and S.R. Nagel, *ibid.* **57**, 1971 (1998).